Int. J. Solids Structures, 1968, Vol. 4, pp. 675 to 688. Pergamon Press. Printed in Great Britain

DIRECT NUMERICAL DETERMINATION OF STRESSES IN ELASTIC SOLIDS AS ILLUSTRATED BY THE TORSION PROBLEM*

JAY W. FELDMANN†

University of California, San Diego, La Jolla, California

Abstract—Using Saint-Venant's torsion problem for purposes of illustration, this paper presents a method for the direct determination of stresses in an elastic solid. The method is compared to finite difference techniques for the determination of the stress function. For a comparable numerical effort, the new method is shown to yield superior results.

1. INTRODUCTION

CURRENT numerical methods of treating problems in elastostatics may be classified as finite difference or finite element methods. Although their original conceptual bases are distinct, these methods can be made to yield identical numerical results. This can be shown by deriving each method as a Ritz type application of the principle of minimum potential energy [1]. When viewed in this manner, the finite element method is equivalent to the finite difference technique; it will therefore not be discussed further in this paper.

Whereas finite difference methods could, in principle, be devised for treating either the differential equations of the displacement field (Navier equations) or those of the stress field (Beltrami–Michell equations), the second possibility has not yet been seriously exploited. Finite difference equations for a field of plane elastic stress have been derived by Prager [2], but numerical experience concerning the advantages or disadvantages of this approach has not yet been accumulated. When interest focuses on stresses rather than displacements, finite difference equations for appropriate stress functions (e.g., Prandtl's stress function in the torsion problem) are generally used rather than finite difference equations for the stress components themselves. For a given mesh size, the use of stress functions might at first glance appear preferable to the use of stress components, because the first procedure involves fewer unknowns. It must be kept in mind, however, that the desired quantities are stresses, that is, appropriate combinations of derivatives of stress functions. To achieve a desired accuracy in the stress components in this manner, a much finer grid must be used than to achieve a comparable accuracy in the values of the stress functions. It is therefore entirely possible that, in the direct numerical determination of stress components, the disadvantages of a greater number of unknowns may be offset by the advantages of the use of a coarser grid. It is the purpose of this paper to show that this is indeed the case, at least as far as Saint-Venant's torsion problem is concerned.

* This study forms part of a research project on methods of stress analysis sponsored at the University of California, San Diego, by the Office of Naval Research, Washington, D.C., under Contract N00014-67-A-0109-0003, Task NR 064-496.

† NASA Trainee, Department of the Aerospace and Mechanical Engineering Sciences.

provided the finite difference equations for Prandtl's stress function are set up in the customary manner. The extension of the method discussed in this paper to other problems in linear elasticity will be the subject of a follow-up paper.

2. BASIC RELATIONS

In this paper, the proposed method will be discussed in the context of Saint-Venant's torsion problem ([3], pp. 258–315). With respect to a system of rectangular Cartesian coordinates x, y in the typical cross-sectional plane, the state of stress at the point x, y is specified by the shearing stresses $\tau_x(x, y)$, $\tau_y(x, y)$, which satisfy the condition of equilibrium†

$$\frac{\partial \tau_x}{\partial x}+\frac{\partial \tau_y}{\partial y} = 0. \tag{1}$$

The equation of compatibility for the corresponding shear strains furnishes a second equation for the shearing stresses, namely

$$\frac{\partial \tau_x}{\partial y}-\frac{\partial \tau_y}{\partial x} = -2G\theta, \tag{2}$$

where G is the shear modulus and θ the angle of twist per unit length. Finally, the condition that the lateral surface of the rod is free of surface tractions yields the boundary condition

$$\nu_x\tau_x+\nu_y\tau_y = 0. \tag{3}$$

where ν_x, ν_y are the components of the unit vector along the exterior normal to the boundary of the cross section.

The equation of equilibrium (1) is identically satisfied if the shearing stresses are derived from Prandtl's stress function $\varphi(x, y)$ in accordance with $\tau_x = \partial\varphi/\partial y$, $\tau_y = -\partial\varphi/\partial x$. The equation of compatibility (2) and the boundary condition (3) then furnish the differential equation

$$\frac{\partial^2\varphi}{\partial x^2}+\frac{\partial^2\varphi}{\partial y^2} = -2G\theta \tag{4}$$

with

$$\varphi = 0 \tag{5}$$

on the boundary of the cross section which is assumed to be simply connected.

3. FINITE DIFFERENCE TREATMENT

Results obtained by finite difference techniques and the new method will be compared with each other for the square and the equilateral triangle, because the exact solutions for these cross sections are available ([3], p. 277 and p. 266).

† Following Nadai ([4], p. 490), the notation τ_x, τ_y is used as a convenient abbreviation for the customary τ_{xz}, τ_{yz}.

3.1 *The square*

Due to symmetry, only the first octant of the x, y plane (shaded in Fig. 1) needs to be considered. For a particular mesh size $h = a/n$ (where n is an integer), the nodes are suitably numbered and the Poisson partial differential equation (3) is replaced by the well-known ([5], p. 111) finite difference equation

$$\varphi_1+\varphi_2+\varphi_3+\varphi_4-4\varphi_0 = -2G\theta h^2, \tag{6}$$

where nodes 1 through 4 are immediately above, below, to the right and to the left of node 0. This equation may be written for each of the m interior nodes in the shaded octant. At nodes on the boundary of the square, $\varphi = 0$.

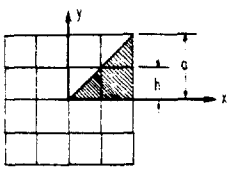

FIG. 1. Square covered by square grid.

As is well known, the maximum shearing stresses occur at the centers of the sides. For sufficiently small h, the stress function varies nearly linearly between adjacent nodes so that, approximately,

$$\tau_{max} = \tau_y(a, 0) = -\frac{\partial\varphi}{\partial x}\bigg|_{(a,0)} = \frac{n}{a}\varphi(a-h, 0), \tag{7}$$

since $\varphi(a, 0) = 0$. Column 1 of Table 1 gives the values of τ_{max} obtained in this manner for several values of n. Note that the analysis involves two approximations: a finite difference equation is substituted for the differential equation and piecewise linear variation of the stress function is assumed to evaluate the finite difference equivalent of the derivative of the stress function. Better results may be obtained by improving on one or both of these approximations.

A convenient Hermitian finite difference expression for the Laplacian operator with a higher degree of precision ([6], p. 101) than that of equation (6) is given by Collatz ([7], p. 542):

$$\nabla^2\varphi_{0,0} = \frac{1}{12h^2}[-40\varphi_{0,0}+8(\varphi_{1,0}+\varphi_{0,1}+\varphi_{-1,0}+\varphi_{0,-1}) + 2(\varphi_{1,1}+\varphi_{-1,1}+\varphi_{-1,-1}+\varphi_{1,-1})]. \tag{8}$$

Here, the subscripts j, k indicate the position of a node with respect to the node 0, 0 for which the finite difference equivalent of (4) is written. Values of τ_{max} obtained from the substitution of (8) into (4) and differentiation based on assumed linear variation of φ between adjacent nodes are shown in Column 3 of Table 1. The improvement over the values in Column 1 is disappointingly small.

Numerical differentiation based on higher-order interpolation should improve the results obtained so far. From the values of the stress function at nodes on the x-axis and the knowledge that (along this axis) the stress function is even in x, it is possible to construct a polynomial $\varphi = \varphi(x^2)$ that assumes the computed values at the nodes. Evaluation of its

TABLE 1. TORSION OF SQUARE RESULTS FOR τ_{max} $G\theta a$

Column		1	2	3	4		5	6
Number of unknowns	n	Finite difference technique				n	New method analysis	
		"Customary" equation		Hermitean equation			Linear	Higher order
		Linear interpol.	Higher order interpol.	Linear interpol.	Higher order interpol.			
1	1	0·500	1·000	0·600	1·200	1	2·000	—
3	2	0·875	1·250	0·918	1·312	—	—	—
4	—	—	—	—	—	2	1·333	1·341
6	3	1·026	1·329	1·048	1·353	—	—	—
9	—	—	—	—	—	3	1·429	1·353
10	4	1·105	1·339	1·118	1·353	—	—	—
16	—	—	—	—	—	4	1·344	(see text)
Exact value	1·351([3], p. 277)							

derivative at $x = a$ then yields τ_{max}. The results of applying this higher-order interpolation to both the customary and the Hermitean finite difference equations for several mesh sizes are given in Columns 2 and 4, respectively, of Table 1. It is seen that the use of higher order interpolation improves the results more than the use of a finite difference approximation with a higher degree of precision.

3.2 *The equilateral triangle*

On account of symmetry, only the shaded triangle in Fig. 2 needs to be considered.

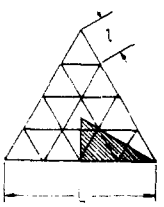

FIG. 2. Equilateral triangle covered by triangular grid.

Collatz ([7], p. 544) gives a finite difference approximation to the Laplacian operator for a triangular grid. From this there results the finite difference equation

$$\frac{2}{3l^2}(\varphi_1+\varphi_2+\varphi_3+\varphi_4+\varphi_5+\varphi_6-6\varphi_0) = -2G\theta \tag{9}$$

where nodes 1 through 6 surround the central node 0. This finite difference equation may be written for each interior node in the shaded triangle. The solution of the resulting linear equations yields approximate values of the stress function at the interior nodes. Once again, linear interpolation may be used to calculate the maximum stress (see equation (7)) and the results for a few mesh sizes are given in Table 2.

It should be noted that there actually are two families of grids, for even and odd n. The first family does not provide a node on the axis of symmetry that is in close proximity to the maximum stress point (center of edge). Therefore either the rough idea of treating φ as practically constant along a normal to and in the vicinity of the center line must be used or some interpolation must be performed to determine the value of φ along the center line, thus getting an improved result (both "rough" and "improved" values for $n = 4$ are given in Table 2). To avoid these difficulties, odd values of n have been preferred in Table 2.

It is worth noting that, for the Poisson equation with constant right-hand side, the Hermitean difference approximation yields again equation (9).

When higher-order interpolation is used in the numerical determination of the derivative of the stress function, it is found that the exact value of τ_{max} is obtained regardless of mesh length. This at first glance startling result is explained by the remark that the stress function for the problem on hand is a cubic polynomial in x and y ([8], p. 322). The expression for the error of the approximation (9) starts with a term in h^2, which vanishes for the present problem: the next error term is proportional to h^4 and involves sixth order derivatives of φ. Accordingly, (9) furnishes exact values of the present cubic stress function, and the discrepancy between the exact value of τ_{max} and the values in Table 2 is entirely due to the error of the numerical differentiation based on linear interpolation. Since for

TABLE 2. TORSION OF EQUILATERAL TRIANGLE RESULTS FOR $\tau_{max}/G\theta L$

Number of unknowns	n	Finite difference technique	n	New method
1	4	0·216 ("rough") 0·243 ("improved") see text	1	0·289
2	5	0·277	—	—
4	7	0·319	3	0·416
9	—	—	5	0·427
Exact value	0·433 ([3], p. 266)			

$n \geq 4$ the higher order interpolation used in this problem is at least cubic, the exact value of τ_{max} must be obtained. Of course, the fact that an exact solution is obtained in this particular case is of limited interest because the stress function is not, in general, a polynomial.

Inspection of the results of the finite difference analysis shows again an indicated convergence to the exact value with decreasing mesh size.

4. NEW NUMERICAL TREATMENT

The complete formulation of the torsion problem in terms of stress components consists of the equilibrium equation (1) and compatibility equation (2) with boundary conditions given by equation (3). If the considered section is covered by a grid, the x and y components of the shear stress at each node may be taken as the unknowns to be determined. Note that equation (3) reduces to one the number of unknown stress components

at boundary nodes while both components vanish at a corner node. For a symmetric cross section, the number of unknown stress components is further reduced by symmetry conditions.

Due to symmetry, only the meshes in the shaded region of Figs. 1 or 2 need to be considered. To each of these meshes overall conditions of equilibrium and compatibility will be applied.

Denoting the components of the unit exterior normal vector to the mesh boundary by n_x and n_y and applying Gauss' theorem to the integral of the equilibrium equation (1) over the mesh area A, we find

$$\int_A \left(\frac{\partial \tau_x}{\partial x}+\frac{\partial \tau_y}{\partial y}\right) \mathrm{d}A = \int_S (n_x\tau_x+n_y\tau_y)\,\mathrm{d}s = 0, \tag{10}$$

where $\mathrm{d}s$ denotes the line element of the mesh boundary S.

Similarly, application of Gauss' theorem to the integral of the compatibility equation (2) over the mesh area A yields

$$\int_A \left(-\frac{\partial \tau_y}{\partial x}+\frac{\partial \tau_x}{\partial y}\right) \mathrm{d}A = \int_S (-n_x\tau_y+n_y\tau_x)\,\mathrm{d}s = -\int_A 2G\theta\,\mathrm{d}A = -2G\theta A \tag{11}$$

since $G\theta$ is independent of x and y. If the components of the unit tangent vector to the mesh boundary that corresponds to a counter-clockwise motion around the mesh are denoted by t_x, t_y, then $n_x = t_y, n_y = -t_x$. Equation (11) may therefore be written as

$$\int_S (t_y\tau_y+t_x\tau_x)\,\mathrm{d}s = 2G\theta A. \tag{12}$$

Equations (10) and (12) will be called the *overall* conditions of equilibrium and compatibility for the considered mesh. A stress field that satisfies these equations for all meshes of a grid will be described as statically and kinematically admissible for this grid. Whereas the true elastic stress field is statically and kinematically admissible *for any grid* with which the cross section may be covered, a stress field that is statically and kinematically admissible *for a given grid* may differ from the true stress field. This difference, however, tends to disappear as the mesh size is decreased indefinitely.

One way of using the overall conditions of equilibrium and compatibility in a numerical method to obtain an approximation to the stress field for a given cross section would be to (i) assume polynomial expressions for τ_x and τ_y that already satisfy all symmetry conditions and (ii) determine the remaining coefficients of these polynomials to satisfy the overall conditions of equilibrium and compatibility for a grid with an appropriate number of meshes. This method is similar to the well-known collocation method (see [7], p. 29) but replaces local equilibrium and compatibility at a finite number of points by overall equilibrium and compatibility for a finite number of meshes.

As a rule, it is, however, more convenient to operate directly with the numerical values of the stress components at discrete grid points rather than with polynomials (or other functions) of x and y that are supposed approximately to describe the stress field over the entire cross section. Now, the integral of, say, the normal component of the shearing stress along a mesh side is completely specified by the values of this component at the endpoints of the side only if the intensity of the stress component varies linearly along the side. The value of the integral is then given by the trapezoidal rule. In the following, this utilization

of the trapezoidal rule is termed "linear analysis". In general, however, numerical overall conditions of equilibrium and compatibility based on the trapezoidal rule are approximations that increase in accuracy with decreasing mesh size. In the following, when nonlinear stress distributions are considered via higher-order quadrature formulas, it will be termed "higher-order analysis".

The following discussion of the square and equilateral triangular cross sections illustrates the method.

4.1 *The square*

In Fig. 3, which corresponds to $n = 2$, the unknown stress components have been identified by letters at all nodes and full use of symmetry conditions has been made.

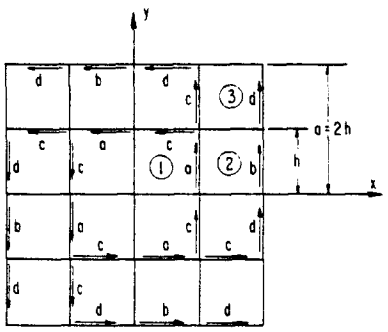

FIG. 3. Square for $n = 2$ with stress components displayed.

Consider, for instance, the mesh labeled 1. At its lower left corner, symmetry requires that $\tau_x = \tau_y = 0$. At its lower right corner, $\tau_x = 0$ by symmetry and the value of τ_y is denoted by a. Symmetry then requires that $\tau_x = -a$, $\tau_y = 0$ at the upper left corner. Finally, symmetry requires $-\tau_x = \tau_y = c$ at the upper right corner. This leaves four unknowns, a through d, the value b being τ_{max}, which is of primary interest.

The three relevant meshes are numbered 1, 2, and 3. Application of the overall condition of equilibrium (10) to mesh 2 in the linear analysis furnishes the equation

$$a+b-2c-d = 0. \tag{13}$$

On account of the symmetries of the stress field, the corresponding equations for meshes 1 and 3 are found to be automatically satisfied.

With the mesh area $A = h^2$, the overall condition of compatibility (12) furnishes the following equations for the meshes 1, 2 and 3 in the linear analysis:

$$\begin{aligned} 2a \quad &+2c \quad &&= 4G\theta h \\ -a+b \quad &+ \quad d &&= 4G\theta h \\ &-2c+2d &&= 4G\theta h. \end{aligned} \tag{14}$$

Solution of the four equations in (13) and (14) yields values for the four unknown shear stress components and in particular

$$b = \tau_{max} = \tfrac{8}{3}G\theta h = \tfrac{4}{3}G\theta a = 1{\cdot}333G\theta a.$$

Since the exact value is 1·351 $G\theta a$, this result is very good, considering the small amount of calculation required to obtain it. (It turns out, however, that the result for this particular case is somewhat fortuitous.)

We now use the same grid but allow the stresses to vary non-linearly between nodes, i.e., apply "higher-order analysis". We begin by observing that along all grid lines both components of stress are either even or odd in the coordinates x, y. Since equations (10) and (12) involve integrations of stress components along grid lines, appropriate quadrature formulas are readily developed.

For an *even* function $f(s)$ that vanishes at $s = 2$, set

$$I = \int_0^1 f \, ds = \alpha f_0 + \beta f_1,$$

$$J = \int_1^2 f \, ds = \gamma f_0 + \delta f_1,$$

where f_0 and f_1 are the values of $f(s)$ at $s = 0$ and $s = 1$, respectively. Using the test functions $f = 4 - s^2$ and $f = 16 - s^4$ to evaluate the coefficients α through δ results in

$$I = \frac{57}{90} f_0 + \frac{34}{90} f_1 \quad \text{and} \quad J = -\frac{33}{90} f_0 + \frac{94}{90} f_1.$$

Similarly, for an odd function $g(s)$, set

$$K = \int_0^1 g \, ds = \varepsilon g_1 + \zeta g_2,$$

$$L = \int_1^2 g \, ds = \eta g_1 + \varkappa g_2,$$

and use the test functions $g = s$ and $g = s - s^3$ to obtain

$$K = \frac{14}{24} g_1 - \frac{1}{24} g_2 \quad \text{and} \quad L = \frac{18}{24} g_1 + \frac{9}{24} g_2.$$

Application of the overall condition of equilibrium (10) to mesh 2 and use of these quadrature formulas yields

$$18a + 9b - 32c - 8d = 0$$

while use of these quadrature formulas in the overall condition of compatibility (12) for the meshes 1, 2 and 3 provides

$$\begin{aligned} 57a \qquad + 34c \qquad &= 90G\theta h \\ -90a + 57b + 60c + 34d &= 180G\theta h \\ 33a - 33b - 94c + 94d &= 90G\theta h. \end{aligned}$$

The four equations just obtained yield

$$b = \tau_{max} = 1{\cdot}341 G\theta a.$$

While this is closer to the true value 1·351 than the value 1·333 obtained by the linear analysis, the amount of improvement is disappointing considering the additional work

required. This appearance, however, is misleading because the value obtained by the linear analysis is fortuitously good in this case. For other cases, the improvement resulting from this approach amply justifies the additional work.

The results of the studies for various mesh sizes for both linear and higher-order analyses are given in Columns 5 and 6, respectively, of Table 1. Inspection of these values shows that the excellent result obtained for $n = 2$ by linear analysis was indeed fortuitous, in as much as the next finer mesh ($n = 3$) gives a *poorer* result.

When all the results for the linear analysis are considered, it is evident that these results form a rapidly converging oscillatory approach to the true value of τ_{max}. Note that the higher-order analysis does improve each result, notably for $n = 3$ where almost the exact value is obtained. For this reason, the higher-order analysis was not carried out for $n = 4$.

Let us now compare the results of the new method with those of the finite difference technique. At first, one might be tempted to make comparisons based on equal mesh sizes (value of n). However, this would be an unfair basis (biased in favor of the new method) since, for a given mesh size, the new method involves, in general, more unknowns than the finite difference method. A much fairer comparison is to look at the results of the two methods in cases involving approximately the same number of unknowns, because this number is a measure of the amount of work required. Table 1 has been arranged with this thought in mind. Comparing Column 5 with Columns 1 and 3, we see that the new linear analysis provides a definite improvement in results over both linear interpolation finite difference techniques, customary and Hermitean (higher degree of precision). Comparing Column 6 with Columns 2 and 4, we see that the higher-order results of the new method are definitely superior to the higher-order interpolation of customary equation results (Column 2) but appear to be just about comparable to the higher-order interpolation of Hermitean equation results (Column 4). Since this latter analysis represented the ultimate in the finite difference technique, it is encouraging that the new method can give comparable results.

However, the main conclusion drawn from these comparisons is that obtained from the more convenient linear analyses: for roughly equivalent amounts of work, the new method gives much more accurate results than the customary finite difference technique.

4.2 *The equilateral triangle*

Figure 2 shows an equilateral triangle of side L with a triangle grid of mesh size $l = L/n$ (in the figure, $n = 4$). We now introduce stresses as unknowns but not as above where the geometry naturally inspired orthogonal components at each node. Instead we introduce the unknown tangential stress components at the center of the sides of all triangular meshes.

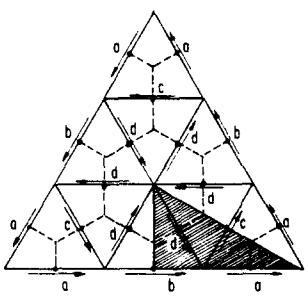

FIG. 4. Triangle for $n = 3$ with stress components displayed.

Figure 4 shows the case $n = 3$, full use of symmetry having been made. The figure shows that only the shaded triangles need to be considered. In addition to the considered grid, we establish a "conjugate" grid formed by the medians of the sides of the triangles. This is the dotted hexagonal grid in Fig. 4.

We now consider overall compatibility for the triangular meshes and overall equilibrium for the conjugate hexagonal meshes. The application of the compatibility equation (12) to the triangles of Fig. 4 with the assumption of piecewise linear stress variations (hence unknowns represent mean values of stresses along grid lines) yields

$$2al - cl = 2G\theta A \quad \text{or} \quad 2a - c = \frac{\sqrt{3}}{2} G\theta l,$$

$$c + 2d = \frac{\sqrt{3}}{2} G\theta l, \tag{15}$$

$$\text{and} \quad b - 2d = \frac{\sqrt{3}}{2} G\theta l.$$

Because of symmetry, the simultaneous solution of these three equations fulfills overall compatibility for all triangular meshes in the cross section.

The application of the overall equilibrium equation (10) to the half-hexagons along the boundary in this linear analysis yields

$$a - b + 2c - 2d = 0. \tag{16}$$

Since equilibrium is identically satisfied for the full hexagon at the center and the one-sixth hexagons at the corners, the satisfaction of equation (16) guarantees overall equilibrium for all meshes of the conjugate grid.

Note that for even integer values of n either equilibrium or compatibility cannot be satisfied for all meshes. It is therefore preferable to restrict the present discussion to odd values of n since both overall equilibrium and overall compatibility may then be satisfied for all meshes. In addition, τ_{max} directly appears as one of the unknowns when n is odd.

The approximation introduced in the quadratures involved in establishing overall equilibrium or overall compatibility for an individual mesh consists in interpreting the average stress value along a grid segment as the local stress value at the center of the segment. This would be fully justified if the variation of stress along the considered grid segment was linear. Again, the error involved in this approximation will tend to zero as the mesh size decreases indefinitely.

Solving equations (15) and (16), we find

$$b = \tau_{max} = 0{\cdot}416 G\theta L.$$

This compares quite well with the exact value of $0{\cdot}433 G\theta L$.

As noted previously, any higher-order approximation for the equilateral triangle is unwarranted since it only leads to the exact solution.

The results of this type analysis for a few cases are given in Table 2. Once again, convergence to the true solution with decreasing mesh size is clearly indicated. Comparison with the finite difference results also given in Table 2 again shows a marked improvement in results for roughly equivalent amounts of work.

The equilateral triangle was reanalyzed with a technique similar to that used with the square instead of the conjugate grid approach just presented. It was determined, however, that the conjugate scheme yielded better results (2 unknowns with the first technique yielded the same results as 1 unknown with the conjugate system; for 4 unknowns, the first approach gave 0·397 vs. 0·416 of the conjugate method). Hence, the use of a conjugate grid appears preferable. This suggests that the use of a conjugate grid may also be preferable for the square.

4.3 *Conjugate grid used for the square*

Application of the conjugate grid scheme of the new method to Fig. 5 provides

$$\tau_{max} = 1{\cdot}286G\theta a$$

after a non-linear interpolation (since τ_{max} itself is not one of the unknowns). This is not as good a result as the $1{\cdot}333G\theta a$ obtained in Section 4.1 for the same number of unknowns and based on a fully linear analysis.

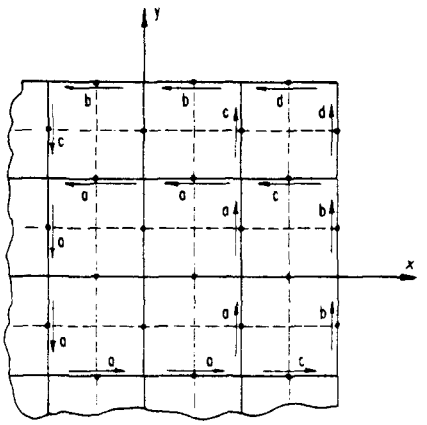

FIG. 5. Square for $n = 2$ with conjugate grid.

Choosing the unknowns as in Fig. 6 so that τ_{max} is included leads to

$$\tau_{max} = 1{\cdot}267G\theta a,$$

an even poorer value.

Since the excellent result obtained in Section 4.1 for 4 unknowns ($n = 2$) was found to be fortuitous, the situation depicted in Fig. 7 was considered. After interpolation, we find

$$\tau_{max} = 1{\cdot}319G\theta a,$$

which is between the two results of Section 4.1, i.e., the linear analysis (1·429) and the higher-order analysis (1·353). Since the work involved here is similarly between those cases (because it is a linear analysis but with a higher-order interpolation), it appears that the degree of accuracy to be expected is directly related to the amount of work expended for both the method presented in Section 4.1 and the conjugate method. The only basis for possibly preferring one method over the other is that the technique of Section 4.1 is somewhat simpler and "natural" for the square and hence might be preferred over the conjugate scheme.

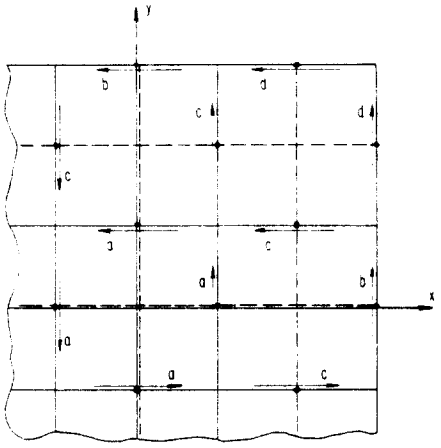

FIG. 6. Square with conjugate grid including τ_{max}.

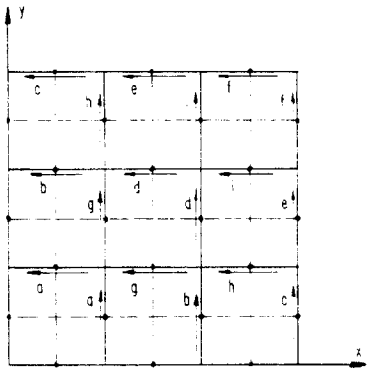

FIG. 7. Square for $n = 3$ with conjugate grid.

5. RELATION OF FINITE DIFFERENCE METHOD TO NEW METHOD

From the preceding section, we may draw a connection between the finite difference and new methods. Consider a square with $n = 2$. The customary finite difference technique, with piecewise linear stress function variation assumed, furnishes the stress components given in Fig. 8.

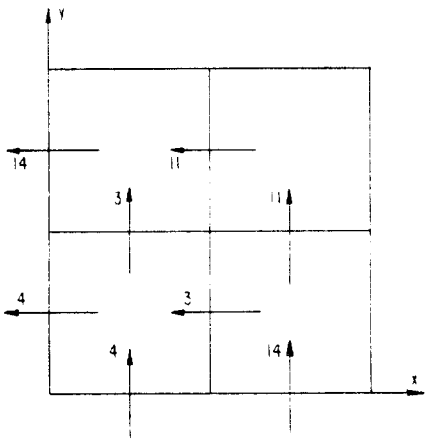

FIG. 8. Stress components furnished by analysis of square (in multiples of $G\theta a/16$).

The solution of the same problem by the conjugate form of the new method provides the same results shown in Fig. 8. With the assumption of piecewise linear variation of the stress function and the linear stress variation assumption "built-in" the conjugate new method, the two methods are completely equivalent. The reason for the superior accuracy claimed for the new method (Tables 1 and 2) lies in the fact that heretofore the interest has been in determining the maximum shearing stress which, for the torsion of the square, is

known to be at the mid-points of the boundary. To obtain the finite difference equivalent to the new method as exhibited by Fig. 6, for instance, requires a modification of the customary finite difference technique, allowing n to be non-integer. Figure 9 shows the grids for the new method (both regular and conjugate are shown solid) and a new finite difference grid (shown dotted) which extends beyond the physical boundary. Since the finite difference

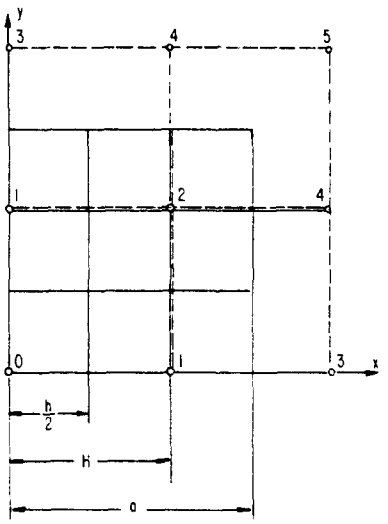

FIG. 9. Square covered by present method (solid) and refined finite difference (dotted) grids.

nodes no longer fall on the boundary (where φ vanishes), it is clear that additional unknowns (i.e., $\varphi_3, \varphi_4, \varphi_5$) have been introduced. Since the stress function vanishes along the boundary, use may be made of the assumption of its linear variation along a grid segment to obtain

$$\varphi_3 = -\varphi_1 \quad \text{and} \quad \varphi_4 = -\varphi_2. \tag{17}$$

Then the customary finite difference technique yields the same stress distribution as the new method of Fig. 6 (e.g., $\tau_{max} = 1{\cdot}267G\theta a$).

This example serves to illustrate that the techniques are indeed equivalent. Although the refined finite difference technique involves fewer unknowns (after relations such as equation (17) are applied), the conjugate new method equations are simple and easily written. In addition, their solution gives the desired quantities (stresses) directly without the further computation required with the finite difference technique.

While the methods are equivalent, it should be borne in mind that the approximations are different. In the finite difference technique, the (exact) partial differential equations are approximated by finite difference expressions and a low order formula is used for numerical differentiation of the stress function. In the new method, equilibrium and compatibility are satisfied regionally rather than pointwise. An approximation enters in the assumption made regarding stress variation so that integration reduces to quadrature. When piecewise linear stress variations are used, it has been shown that the method is completely equivalent to a refined form of the customary finite difference technique.

6. CONCLUSIONS

A new method dealing directly with stress components has been developed in two forms as exemplified by the square and equilateral triangle applications. The latter version, called the conjugate form, has been shown to be equivalent to a refined finite difference technique.

Both forms of the new method yield better results than the customary finite difference technique. Even when the conjugate form is compared with its equivalent refined finite difference technique (i.e., equal accuracies), the new form is still preferred since its equations are set up more readily (even though they involve more unknowns) and their solution directly yields the desired quantities, i.e., the stresses.

It has been shown that the assumption of higher order variation of stresses along grid elements may be incorporated into the new method and that this yields results comparable to the ultimate finite difference technique (higher degree of precision Hermitean equation for the stress function with higher-order interpolation to calculate stresses). However, for arbitrary shapes, higher order techniques become difficult to apply and one must resort to linear analysis, where it has been demonstrated that the new method is preferable.

While this discussion has been limited to the torsion problem, the new method itself is of course not so restricted. Its extension to other applications is worth exploring and work in this direction is in progress.

Acknowledgement—The author is greatly indebted to Professor Prager for guidance and inspiration.

REFERENCES

[1] O. C. ZIENKIEWICZ and Y. K. CHEUNG, Finite elements in the solution of field problems. *Engineer. Lond.*, 507–570 (24 Sept. 1965).
[2] W. Prager, Direct numerical determination of the stress field in a thin elastic disk. *Z. angew. Math. Phys.* **18**, 301–311 (1967).
[3] S. TIMOSHENKO and J. N. GOODIER, *Theory of Elasticity*. McGraw-Hill (1951).
[4] A. NADAI, *Theory of Flow and Fracture of Solids*, Vol. 1. McGraw-Hill (1950).
[5] C. WANG, *Applied Elasticity*. McGraw-Hill (1953).
[6] W. PRAGER, *Introduction to Basic FORTRAN Programming and Numerical Methods*. Blaisdell (1965).
[7] L. COLLATZ, *The Numerical Treatment of Differential Equations*, 3rd edition, translated by P. G. Williams. Springer (1960).
[8] A. E. H. LOVE, *A Treatise on the Mathematical Theory of Elasticity*, 4th edition. Dover (1944).

(*Received* 26 *December* 1967; *revised* 15 *January* 1968)

Абстракт—Используя для иллюстрации задачу кручения Сен Венана, настоящая работа представляет метод прямого определения напряжений в упругом твердом теле. Этот метод сравнивается с задачей в конечных разностях, для определения функции напряжения. Чтобы показать трудоемкость сравниваемого расчета, новый метод указывает возможность получения лучших результатов.